Searching for invisibly decaying Higgs bosons at CERN LEP II

F. de Campos,[1,*] O. J. P. Éboli,[2,†] J. Rosiek,[1,3,‡] and J. W. F. Valle,[1,§]
[1]*Instituto de Física Corpuscular - Consejo Superior de Investigaciones Cientificas, Departmento de Física Teòrica, Universitat de València 46100 Burjassot, València, Spain*
[2]*Physics Department, University of Wisconsin, Madison, Wisconsin 53706*
[3]*Institut für Theoretische Physik, Universität Karlsruhe, Postfach 6980, 76128 Karlsruhe, Germany*
(Received 26 June 1996)

We study the potential of CERN LEP II to unravel the existence of invisibly decaying Higgs bosons, predicted in a wide class of models. We perform a model-independent analysis, focusing our attention on the final state topologies exhibiting $b\bar{b}$ or $\ell^+\ell^-$ ($\ell=\mu$ or e) pairs and missing energy. We carefully evaluate the signals and backgrounds, choosing appropriate cuts to enhance the discovery limits. Our results demonstrate that LEP II is capable of discovering such a Higgs boson for a wide range of masses and couplings. [S0556-2821(97)01601-9]

PACS number(s): 14.80.Cp, 12.60.Fr

I. INTRODUCTION

The problem of mass generation constitutes one of the main puzzles in particle physics. It is believed that spontaneous breaking of gauge symmetry through the expectation value of a scalar SU(2)⊗U(1) doublet is the origin of the masses of the fermions as well as those of the gauge bosons. The key implication for this scenario is the existence of the Higgs boson [1], not yet found. The first round of e^+e^- collision experiments at th e CERN e^+e^- collider LEP have constrained the standard model Higgs boson mass to $m_h \gtrsim 65$ GeV [2]. The second phase of LEP will probe the electroweak-breaking sector in a new energy region and this is very interesting both from the point of view of the standard model (SM) as well as its extensions.

A large variety of well-motivated extensions of the SM Higgs sector are characterized by the spontaneous violation of a global U(1) lepton number symmetry by an SU(2)⊗U(1) singlet vacuum expectation value $\langle\sigma\rangle$ [3]. In general, these models contain additional Higgs bosons, as well as a massless Goldstone boson, called Majoron (J), which interacts very weakly with normal matter, and has been postulated in order to give mass to neutrinos in various different contexts [4]. It is specially interesting for our purposes to consider those models where such symmetry is broken at the electroweak scale or below, i.e., $\langle\sigma\rangle \lesssim 1$ TeV [5]. Although the interactions of the Majoron with quarks, leptons, and gauge bosons is naturally very weak, as required by astrophysics [6], it can have a relatively strong interaction with the Higgs boson. In this case the main Higgs boson decay channel is likely to be ''invisible'': e.g.,

$$h \to JJ, \tag{1}$$

where J denotes the Majoron field. This feature also appears in variants of the minimal supersymmetric model in which R parity is broken spontaneously [7]. Notwithstanding, our discussion is not limited to Majoron models since invisibly decaying Higgs bosons also appear in other models [8]. For instance, in the minimal supersymmetric standard model with conserved R parity, the Higgs boson can decay invisibly into the lightest neutralino pair depending on the choice of the parameters.

The invisible Higgs boson decay leads to events with large missing energy that could be observable at LEP II and affect the Higgs boson discovery limits. In particular, the invisible decay could contribute to the signal of two acoplanar jets or leptons plus missing momentum. This feature of invisible Higgs boson models allows one to strongly constrain the Higgs boson mass in spite of the fact that the model involves new parameters compared to the ones of the SM. In particular, the LEP I limit on the predominantly doublet Higgs boson mass is close to the SM limit irrespective of the decay mode of the Higgs boson [10,11].

In the next section, we discuss the parameterization of Higgs boson couplings relevant for their production at LEP. Section III contains a detailed presentation of the expected Higgs boson signals as well as SM backgrounds in the framework of a two-doublet model, which contain both the Zh as well as Ah production channels. Sec. IV contains a discussion of the Higgs boson discovery limits at LEP II for the various topologies considered in Sec. III and for different LEP II center-of-mass energies. In the last section we present a brief overall discussion of the phenomenological implications.

II. PARAMETRIZATION OF HIGGS BOSON PRODUCTION AND DECAYS

In order to motivate our choice for the Higgs boson effective interactions, we consider a model containing two Higgs

*Electronic address: fernando@flamenco.ific.uv.es
†Permanent address: Instituto de Física, Universidade de São Paulo, C.P. 66318, CEP 05389-970 São Paulo, Brazil. Electronic address: eboli@phenom.physics.wisc.edu
‡On leave of absence from Institute for Theoretical Physics, University of Warsaw. Electronic address: rosiek@fuw.edu.pl, rosiek@itpaxp3.physik.uni-karlsruhe.de
§Electornic address: valle@flamenco.ific.uv.es

doublets ($\phi_{1,2}$) and a singlet (σ) under the SU(2)⊗U(1) group. The singlet Higgs field carries a nonvanishing global lepton number charge. The scalar Higgs potential of the model can be specified as

$$V=\mu_i^2\phi_i^\dagger\phi_i+\mu_\sigma^2\sigma^\dagger\sigma+\lambda_i(\phi_i^\dagger\phi_i)^2+\lambda_3(\sigma^\dagger\sigma)^2+\lambda_{12}(\phi_1^\dagger\phi_1)\times(\phi_2^\dagger\phi_2)+\lambda_{13}(\phi_1^\dagger\phi_1)(\sigma^\dagger\sigma)+\lambda_{23}(\phi_2^\dagger\phi_2)(\sigma^\dagger\sigma)+\delta(\phi_1^\dagger\phi_2)(\phi_2^\dagger\phi_1)+\tfrac{1}{2}\kappa[(\phi_1^\dagger\phi_2)^2+\text{H.c.}], \quad (2)$$

where the sum over repeated indices i (=1,2) is assumed.

For appropriate choice of parameters, the minimization of the above potential leads to the spontaneous breaking of the SU(2)⊗U(1) gauge symmetry, as well as the global $U(1)_L$ symmetry. This allows us to identify a total of three massive CP-even scalars $H_i(i=1,2,3)$, plus a massive pseudoscalar A and the massless Majoron J.[1] For definiteness we assume that at the LEP II energies only three Higgs particles can be produced: the lightest CP-even scalar h, the CP-odd massive scalar A, and the massless pseudoscalar Majoron J. Notwithstanding, our analysis is also valid for the situation where the Higgs boson A is absent [12], which can be obtained by setting the couplings of this field to zero.

At LEP II, the main production mechanisms of invisible Higgs boson are the Bjorken process ($e^+e^-\to hZ$) and the associated production of Higgs bosons pairs ($e^+e^-\to Ah$), which rely upon the couplings hZZ and hAZ, respectively. An important feature of the above model is that the Majoron is a singlet under SU(2)⊗U(1) and possesses feeble couplings to the gauge bosons, thus evading strong LEP I constraints coming from the invisible Z width. The hZZ and hAZ interactions can be expressed, without loss of generality, in terms of the two parameters ϵ_A and ϵ_B:

$$\mathcal{L}_{hZZ}=\epsilon_B(\sqrt{2}G_F)^{1/2}M_Z^2Z_\mu Z^\mu h, \quad (3)$$

$$\mathcal{L}_{hAZ}=-\epsilon_A\frac{g}{\cos\theta_W}Z^\mu h\overleftrightarrow{\partial}\mu A, \quad (4)$$

with $\epsilon_{A(B)}$ being determined once a model is chosen. For instance, in the framework of the minimal SM $\epsilon_A=0$ and $\epsilon_B=1$, while a Majoron model with one doublet and one singlet leads to $\epsilon_A=0$ and $\epsilon_B^2\leqslant 1$. In the framework of the minimal supersymmetric standard model $\epsilon_{A(B)}$ are functions of the parameters defining this model.

The signatures of the Bjorken process and the associated production depend upon the allowed decay modes of the Higgs bosons h and A. For Higgs boson masses m_h accessible at LEP II energies the main decay modes for the CP-even state h are $b\bar{b}$ and JJ. We treat the branching fraction B for $h\to JJ$ as a free parameter. In most models B is basically unconstrained and can vary from 0 to 1. Moreover, we also assume that, as it happens in the simplest models, the branching fraction for $A\to b\bar{b}$ is nearly one, and the invisible A decay modes $A\to hJ$, $A\to JJJ$, although CP allowed, do not exist. Therefore, our analysis depends finally upon five parameters: M_h, M_A, ϵ_A, ϵ_B, and B. This parametrization is quite general and very useful from the experimental point of view since limits on M_h, M_A, ϵ_A, ϵ_B, and B can be later translated into bounds on the parameter space of many specific models.

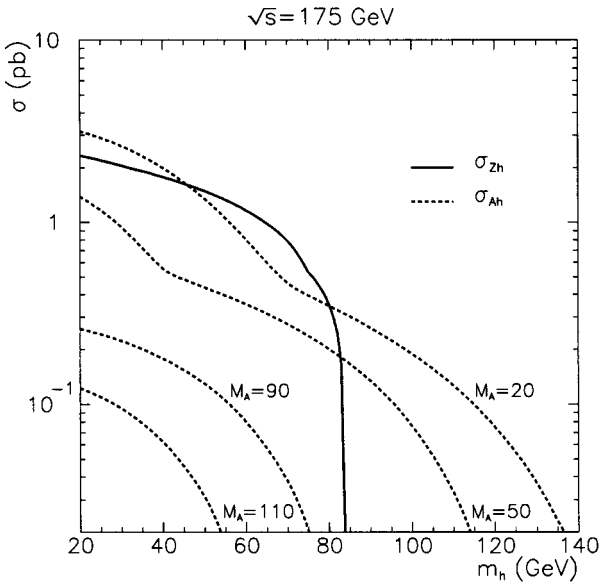

FIG. 1. Total cross section for the production of invisibly decaying Higgs bosons through the Bjorken (solid line) and associated production (dotted line) mechanisms at $\sqrt{s}=175$ GeV.

The parameters defining the general hZZ and hAZ interactions can be constrained by the LEP I data. In fact, Refs. [10,13] analyze some signals for invisibly decaying Higgs bosons, and conclude that LEP I excludes M_h up to 60 GeV provided that $\epsilon_B>0.4$. In what follows we extend the analysis to the energies that will be available at LEP II.

III. SIGNATURES AND BACKGROUNDS

In this work,[2] we focus our analysis in the following signals for the production of invisibly decaying Higgs bosons h:

$$e^+e^-\to(Zh+Ah)\to b\bar{b}+\not{p}_T, \quad (5)$$

$$e^+e^-\to Zh\to\ell^+\ell^-+\not{p}_T, \quad (6)$$

where ℓ stands for e or μ. The signal (6) was previously analyzed in Refs. [10,12]. At LEP II energies the W-fusion process ($e^+e^-\to\nu_e\bar{\nu}_e h$) leads not only to a negligible contribution to the Higgs boson production cross section but also to an unidentifiable final state, since $h\to JJ$, and consequently, we will not take this reaction into account. We exhibit in Fig. 1 the total cross section for the production of Zh and Ah pairs before the introduction of cuts, assuming that $\epsilon_A=\epsilon_B=1$. It is interesting to note that the associated production dominates over the Bjorken mechanism for

[1]For simplicity, we assume throughout this paper that CP is conserved in the scalar sector.

[2]Partial results of our analysis [14] appeared in the proceedings of the ''Physics at LEP II'' workshop [9].

$M_A < M_Z$. This effect is further enhanced by the large branching fraction of A going into b-quark pairs and of h going to JJ.

For the sake of completeness, we also include the channels where h decays visibly into a $b\bar{b}$ quark pair

$$e^+e^- \to Zh \to \ell^+\ell^- + b\bar{b}, \tag{7}$$

$$e^+e^- \to (Zh + Ah) \to b\bar{b} + b\bar{b}, \tag{8}$$

which allows us to obtain additional limits on ϵ_A and ϵ_B. These channels were subject of many detailed analyses performed in the framework of the SM or the two-Higgs doublet model. Thus, we do not repeat them fully here. Instead, we adopt partially the results quoted in Ref. [15] and combine them with our results on the invisible Higgs boson decay channels.

Our goal is to evaluate the limits on M_h, M_A, ϵ_A, ϵ_B, and B that can be obtained at LEP II from the above processes. In order to do so, we study carefully the signals and backgrounds, choosing the cuts to enhance the former. We analyze the signals and backgrounds using the PYTHIA event generator [16], and taking into account the QED (QCD) initial and final state radiation, as well as fragmentation. In order to reconstruct the jets we employ the subroutine LUCLUS of PYTHIA.

A. Topology $b\bar{b}\not{p}_T$

There are three sources of signal events with the topology 2 b jets + $\not{p}_T$: one due to the associated production of Higgs bosons and two due to the Bjorken mechanism:[3]

$$e^+e^- \to (A \to b\bar{b}) + (h \to JJ), \tag{9}$$

$$e^+e^- \to (Z \to b\bar{b}) + (h \to JJ), \tag{10}$$

$$e^+e^- \to (Z \to \nu\bar{\nu}) + (h \to b\bar{b}). \tag{11}$$

In the framework of the SM, there are several sources of background for this topology:[4]

$$e^+e^- \to Z/\gamma Z/\gamma \to q\bar{q}\nu\bar{\nu}, \tag{12}$$

$$e^+e^- \to Z^*/\gamma^* \to q\bar{q}[n\gamma], \tag{13}$$

$$e^+e^- \to [e]\gamma e \to [e]\nu W \to q\bar{q}'[e]\nu, \tag{14}$$

$$e^+e^- \to W^+W^- \to q\bar{q}'[\ell]\nu, \tag{15}$$

$$e^+e^- \to [e^+e^-]\gamma\gamma \to [e^+e^-]q\bar{q}, \tag{16}$$

where the particles in square brackets escape undetected and the jet originating from the quark q is identified (misidentified) as being a b jet. In our analysis, we assume that particles making an angle smaller than 12° with the beam pipe are not detected. The above reactions exhibit two sources of missing momentum: neutrinos and particles going down the beam pipe. Moreover, the final state jets can also lead to missing transverse momentum since we perform a full simulation of the event, allowing for meson and hadron decays that can produce neutrinos or undetected particles. The expected numbers of background events from the processes (12)–(16), before applying the selection cuts, are shown in the Table I.

TABLE I. Expected number of background events in the $b\bar{b}\not{p}_T$ channel before cuts for three values of $\sqrt{s}$ and integrated luminosity $\mathcal{L}$.

$\sqrt{s}$ (GeV)	$\mathcal{L}$ (pb^{-1})	$Z/\gamma Z/\gamma$	Z^*/γ^*	$e\nu W$	W^+W^-	$\gamma\gamma$
175	500	105	5.5×10^4	220	6.4×10^3	2.2×10^3
190	300	209	2.6×10^4	182	4.9×10^3	1.4×10^3
205	300	295	2.2×10^4	237	5.1×10^3	1.5×10^3

At this point the simplest and most efficient way to improve the signal-to-background ratio is to use the fact that the Higgs bosons A and h decay into jets possessing b quarks. So we require that the events contain b-tagged jets. Moreover, the background can be further reduced by demanding a large $\not{p}_T$. Having these facts in mind we impose the following set of cuts, based on the ones used by the DELPHI Collaboration for the SM Higgs boson search [15].

(1) *Missing momentum cuts*. We require the following.

The z component of the missing momentum is smaller than $0.15\times\sqrt{s}$.

The absolute value of the cosine of the polar angle of the missing momentum is less than 0.9. These two cuts are used to reject events whose missing momentum is due to undetected particles going down the beam pipe.

The transversal component of missing momentum $\not{p}_T$ should be bigger than 25 GeV for $\sqrt{s}=175$ and 190 GeV, and 30 GeV for $\sqrt{s}=205$ GeV.

(2) *Acolinearity cut.* The cosine of the angle between the axes of the two most energetic jets is required to be above -0.8. This is equivalent to the requirement that the angle between the jet axes is smaller than 145°. This cut reduces the $Z\to q\bar{q}$ background, where the $\not{p}_T$ originates from neutrinos and jet fluctuations, and consequently it is parallel to the jet thrust axes.

(3) *Scaled acoplanarity cut.* Acoplanarity is defined as the complement of the angle in the plane perpendicular to the beam between the total momenta in the two thrust hemispheres. Scaling the acoplanarity by the minimum of $\sin\theta_{jet\,1}$ and $\sin\theta_{jet\,2}$ [15] avoids instabilities at low polar jet angles. We impose that the scaled acoplanarity is greater than 7°.

(4) *Thrust/number of jets cut.* We require the event thrust to be bigger than 0.8. However, this cut gives relatively small signal efficiency for the process (9) [or (11)] provided M_A (M_h) is in the range 45–80 GeV. Therefore, for this mass range, we demand that the two most energetic jets should carry more than 85% of the visible energy instead of the thrust cut.

(5) *Charged multiplicity cut.* We impose that the event should contain more than eight charged particles. This cut

[3] A similar analysis in the framework of supersymmetric models can be found in pp. 65 and 66 of Ref. [9].

[4] We did not take into account the nonresonant contributions to the process $e^+e^- \to Z\nu\bar{\nu} \to q\bar{q}\nu\bar{\nu}$ since they are small at LEP II energies [17] compared with the resonant process (12).

TABLE II. Suppression factors for the signal and various backgrounds in the $bb\not{p}_T$ channel due to b-tagging cut (based on Table 5 of Ref. [15]).

Signal	$Z/\gamma Z/\gamma$	Z^*/γ^*	$e\nu W$	W^+W^-
68%	16%	14%	1.5%	3.0%

eliminates potential backgrounds from the production of $\tau^+\tau^-$ pairs.

(6) *b-tagging cut.* We accept only the events containing two b-tagged jets. In the analysis, we adopt the efficiencies for the b tagging directly from the DELPHI note [15]: 68% efficiency for the signal and the appropriate values for the backgrounds extracted from Table 5 of Ref. [15] (see Table II).

(7) *Invariant mass cut.* We impose that the total visible invariant mass should be in the range $M \pm 10$ GeV, where M is the mass of the visibly decaying particle (Z, h, or A).

We exhibit in Fig. 2 the expected number of signal events N_A, N_{JJ}, and $N_{\rm SM}$ originating from the production processes (9), (10), and (11), respectively, for $\sqrt{s}=175$ GeV and an integrated luminosity $\mathcal{L}=500$ pb^{-1}. We impose all the above cuts, but the invariant mass one, and assume that $\epsilon_A=\epsilon_B=1$ and that there is no suppression due to the h decay branching ratio (B). Obviously, it is trivial to obtain the number of signal events for arbitrary ϵ_A, ϵ_B, and B from this figure by rescaling our results with appropriate powers of these parameters; see Sec. III below.

The number of background events after applying the above cuts, excluding the invariant mass cut, are shown in Table III. The most important background after the cuts is the production of a Z pair (12), which grows substantially

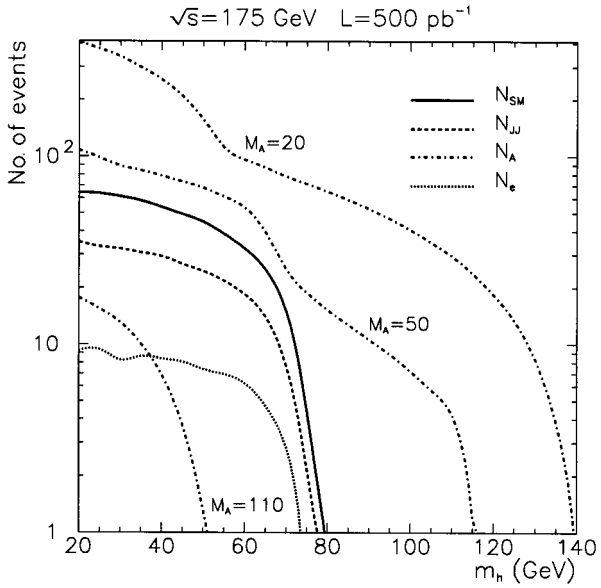

FIG. 2. Expected number of signal events after cuts for the processes $e^+e^-\to(Z\to b\bar{b})+(h\to JJ)$ (N_{JJ}), $e^+e^-\to(Z\to\nu\bar{\nu})+(h\to b\bar{b})$ $(N_{\rm SM})$, $e^+e^-\to(A\to b\bar{b})+(h\to JJ)$ (N_A), and $e^+e^-\to(Z\to e^+e^-)+(h\to b\bar{b})$ (N_e), assuming $\epsilon_A=\epsilon_B=1$ and no suppression due to h decay branching ratios in each case. Note that N_A is given for three choices of M_A values.

TABLE III. Number of the background events in the $b\bar{b}\not{p}_T$ channel after all cuts, but the invariant mass one.

$\sqrt{s}$ (GeV)	$\mathcal{L}$ (pb^{-1})	$Z/\gamma Z/\gamma$	Z^*/γ^*	$e\nu W$	W^+W^-	$\gamma\gamma$	Total
175	500	0.79	0.76	0.46	0.29	0.00	2.31
190	300	1.17	0.44	0.38	0.23	0.00	2.23
205	300	4.26	0.12	0.46	0.19	0.00	5.02

after the threshold for the production of on-shell Z's is reached. Notice that our cuts eliminate completely the large background due to $\gamma\gamma$ reactions.

The backgrounds can be further reduced introducing the visible invariant mass cut. However, depending on the h and A masses, this cut also reduces the signal and weakens the limits on the ZhA and ZZh couplings. Therefore, for each mass combination four limits are calculated: with or without the invariant mass cut and with the thrust cut or the cut on the minimal two-jet energy. The best limit is kept.

B. Topology $\ell^+\ell^-\not{p}_T$

The events with the final state topology $\ell^+\ell^-\not{p}_T$ are generated by the Bjorken process

$$e^+e^-\to(Z\to\ell^+\ell^-)+(h\to JJ), \tag{17}$$

where $\ell=e$ or μ. In this case, the signature is the presence of two charged leptons with an invariant mass compatible with the Z mass, plus missing energy. This topology is the trademark of all models exhibiting invisibly decaying Higgs bosons with sizable couplings to the Z. Notice that the cross section for this process depends only upon ϵ_B, M_h, and B.

We consider only the e^+e^- and $\mu^+\mu^-$ channels because they are cleaner than the $\tau^+\tau^-$ one and their backgrounds are smaller. The possible background sources for this topology are

$$e^+e^-\to Z/\gamma Z/\gamma\to\ell^+\ell^-\nu\bar{\nu}, \tag{18}$$

$$e^+e^-\to Z^*/\gamma^*\to\ell^+\ell^-[n\gamma], \tag{19}$$

$$e^+e^-\to W^+W^-\to\ell^+\ell^-\nu\bar{\nu}, \tag{20}$$

$$e^+e^-\to e\gamma e\to eW\nu\to e^\pm\ell^\mp\nu\bar{\nu}, \tag{21}$$

$$e^+e^-\to[e^+e^-]\gamma\gamma\to[e^+e^-]\ell^+\ell^-. \tag{22}$$

Notice that the background (21) is relevant just for $\ell=e$.

The $\ell^+\ell^-\not{p}_T$ signal shares many features in common with the $b\bar{b}\not{p}_T$ one. First of all, the presence of an invisibly decaying particle leads to missing energy. Furthermore, the two leptons in the final state are either collinear nor in the same plane since this is not a two going into two process. Therefore, in order to enhance the signal, we introduce the following cuts similar to the ones applied for the $b\bar{b}\not{p}_T$ topology:

(1) We require the events to satisfy the same missing momentum cuts employed in Sec. III A; (2) we introduce an acolinearity cut, imposing that the cosine of the angle between the leptons is larger than -0.8; (3) we also demand the scaled acoplanarity of the lepton pair to be greater than

TABLE IV. Numbers of the background events in the $e^+e^-\not{p}_T$ channel. (a) and (b) denote the number of events before and after cuts, respectively. Since the number of events after cuts depends on M_h, we display the maximal values. The backgrounds for the $\mu^+\mu^-\not{p}_T$ channel are identical except for the $e\nu W$ column, which vanishes in this case.

		$Z/\gamma Z/\gamma$		Z^*/γ^*		W^+W^-		$e\nu W$		Total
$\sqrt{s}$ (GeV)	$\mathcal{L}$ (pb^{-1})	(a)	(b)	(a)	(b)	(a)	(b)	(a)	(b)	(b)
175	500	6.4	0.01	4.2×10^3	0.00	74	2.47	232	0.01	2.49
190	300	14	0.14	2.1×10^3	0.00	57	1.03	189	0.02	1.19
210	300	20	1.25	1.7×10^3	0.00	60	0.73	242	0.01	2.00

7°; (4) we require that the event should contain exactly two charged particles identified as electrons or muons; (5) we impose that the invariant mass of the lepton pair should be in the range $M_Z\pm5$ GeV. In addition, we require that the total energy of the lepton pair should be in the range $E_Z(M_h)\pm5$ GeV, where

$$E_Z(M_h)=\frac{s+M_Z^2-M_h^2}{2\sqrt{s}}. \tag{23}$$

These cuts are essential to reduce the WW background. Notice that the invariant mass bin for the lepton pair in this topology is smaller than the one used for the visible mass for the topology $b\bar{b}\not{p}_T$ because the energy and momentum can be better determined for leptons than those for jets.

The expected number of $e^+e^-\not{p}_T$ signal events (N_e) after cuts is also shown for $\sqrt{s}=175$ GeV in Fig. 2. Notice that for a wide range of masses M_h and M_A there are more signal events with the topology $b\bar{b}\not{p}_T$. We exhibit in Table IV the expected number of background events originating from the processes (18)–(21), before and after applying the above cuts. Notice that the most important irreducible background after the cuts is due to process (20). Two photon reactions, process (22), lead to a large number of $\ell^+\ell^-$ pairs (3200, 2080, and 2230 at $\sqrt{s}=$ 175, 190, and 205 GeV, respectively); however, it is completely eliminated by our cuts.

C. Topologies without missing energy

There are three signal processes where the amount of missing energy should be small, up to initial state radiation and jet fluctuations. They are

$$e^+e^-\to(A\to b\bar{b})+(h\to b\bar{b}), \tag{24}$$

$$e^+e^-\to(Z\to b\bar{b})+(h\to b\bar{b}), \tag{25}$$

$$e^+e^-\to(Z\to\ell^+\ell^-)+(h\to b\bar{b}). \tag{26}$$

Therefore, we must consider two new topologies: events with four b-tagged jets ($bbbb$) and events exhibiting two leptons and two b jets ($\ell^+\ell^-b\bar{b}$). These topologies were the subject of many extensive analyses within the framework of the SM and its minimal supersymmetric version [15].

For the sake of completeness, we take into account the signal events originating from processes (24)–(26). However, we only evaluate the total signal cross sections without cuts using the PYTHIA 7.4 generator. In order to study the constraints emanating from these processes we adopt the signal detection efficiencies and the estimated background values quoted in Ref. [15].

It is interesting to point out that the ratio of the number of events with topology $bbbb$ to the ones with $\ell^+\ell^-b\bar{b}$ is independent of B.

TABLE V. Symbols used to denote the number of signal events after cuts in the various channels.

Symbol	Process
$N_{JJ}(M_h)$	$e^+e^-\to(Z\to b\bar{b})+(h\to JJ)$
$N_{\rm SM}(M_h)$	$e^+e^-\to(Z\to\nu\bar{\nu})+(h\to b\bar{b})$
$N_L(M_h)$	$e^+e^-\to(Z\to\ell^+\ell^-)+(h\to JJ)$
$N_{ZH}(M_h)$	$e^+e^-\to(Z\to b\bar{b})+(h\to b\bar{b})$
$N_{ZL}(M_h)$	$e^+e^-\to(Z\to\ell^+\ell^-)+(h\to b\bar{b})$
$N_A(M_h,M_A)$	$e^+e^-\to(A\to b\bar{b})+(h\to JJ)$
$N_{AH}(M_h,M_A)$	$e^+e^-\to(A\to b\bar{b})+(h\to b\bar{b})$

IV. BOUNDS ON INVISIBLY DECAYING HIGGS BOSON COUPLINGS

We define in Table V the symbols used to denote the number of signal events for the different topologies analyzed in the previous section, after imposing the cuts and assuming that $\epsilon_A=\epsilon_B=1$ and that there is no suppression due to the h branching ratio to each final state.

The expected numbers of signal events for the various final state topologies can be expressed as simple combinations of the parameters ϵ_A, ϵ_B, and B and the quantities defined in Table V, which, in turn, depend on the Higgs boson masses (M_h,M_A):

$$N_{bb}(M_h,M_A)=\epsilon_B^2[BN_{JJ}+(1-B)N_{\rm SM}]+\epsilon_A^2BN_A, \tag{27}$$

$$N_{ll}(M_h)=\epsilon_B^2BN_L, \tag{28}$$

TABLE VI. Typical values of the 95% C.L. maximum number of signal events in each channel, assuming that the analysis is done for just one channel.

$\sqrt{s}$ (GeV)	$\mathcal{L}$ (pb^{-1})	$b\bar{b}\not{p}_T$	$\ell^+\ell^-\not{p}_T$
175	500	4.70	6.36
190	300	4.73	4.68
205	300	6.33	5.93

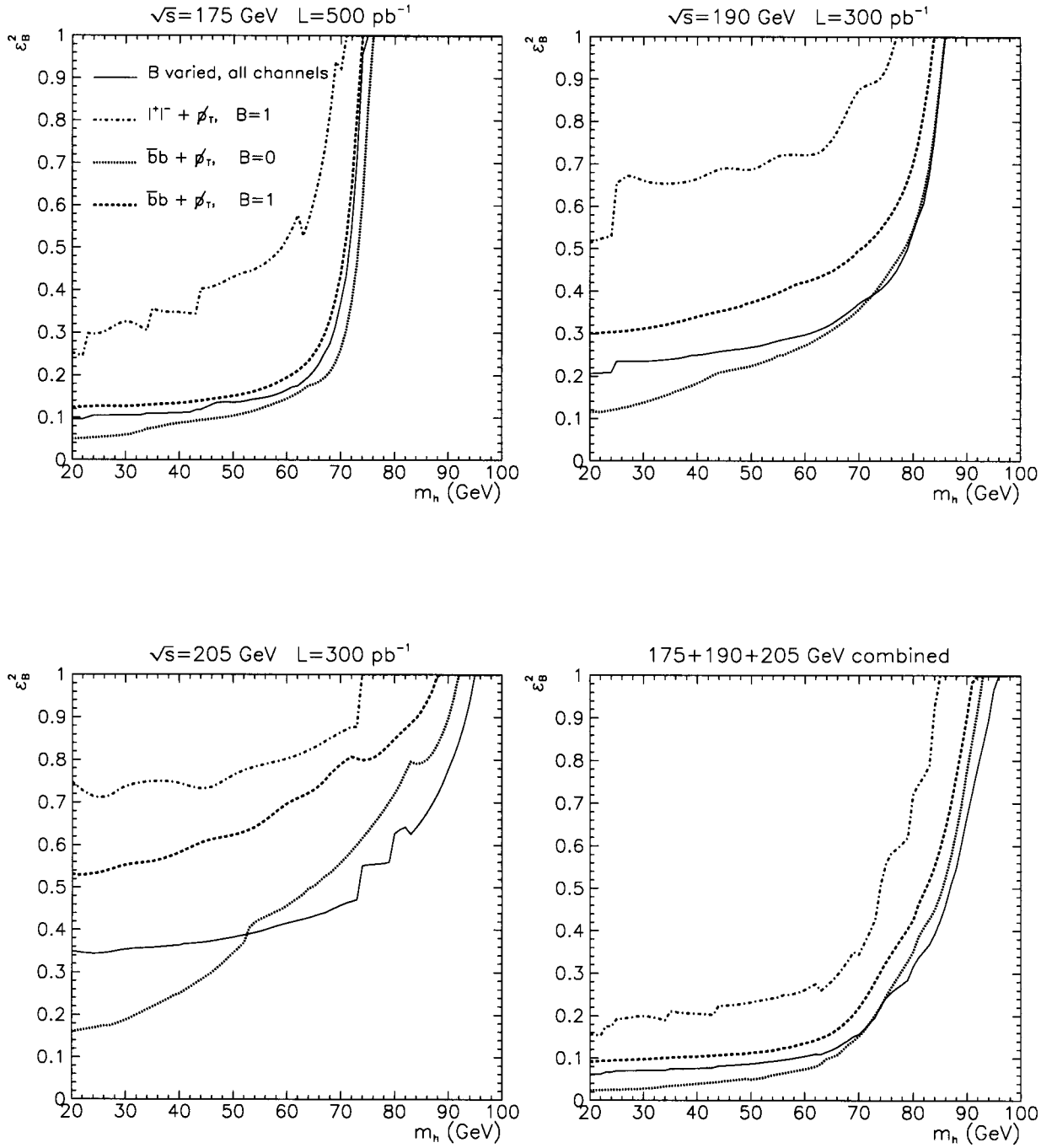

FIG. 3. Bounds on ϵ_B^2 as a function of M_h for three values of $\sqrt{s}$ and the three center-of-mass energies combined. See text for further details.

$$N_{4b}(M_h,M_A)=\epsilon_B^2(1-B)N_{ZH}+\epsilon_A^2(1-B)N_{AH}, \quad (29)$$

$$N_{llbb}(M_h)=\epsilon_B^2(1-B)N_{ZL}, \quad (30)$$

where the quantities N_{bb}, $N_{\ell\ell}$, N_{4b}, and N_{llbb} stand for the number of signal events after cuts for the topologies $bb\not{p}_T$, $\ell^+\ell^-\not{p}_T$, $bbbb$, and $\ell^+\ell^-bb$, respectively. We would like to stress that it is important to consider all the above topologies since the expected numbers of events in the various channels never vanish simultaneously for any value of B, as can be seen from expressions (27)–(30). This allows us to obtain bounds on ϵ_A^2 and ϵ_B^2 couplings without any assumptions on the h decay modes by varying B from 0 to 1 and taking the weakest limits.

In order to access the potentiality of LEP II to unravel the existence of invisibly decaying Higgs bosons we assume that only the background events were observed in accordance with the Tables III and IV. Then, using Poisson statistics, we evaluate the region of the five-dimensional parameter space (M_h, M_A, ϵ_A, ϵ_B, B) that is excluded by this result at 95% confidence level. Since this parameter space is quite large, we make some simplifying assumptions below. For each channel, the general form of the constraints on ϵ_A and ϵ_B is

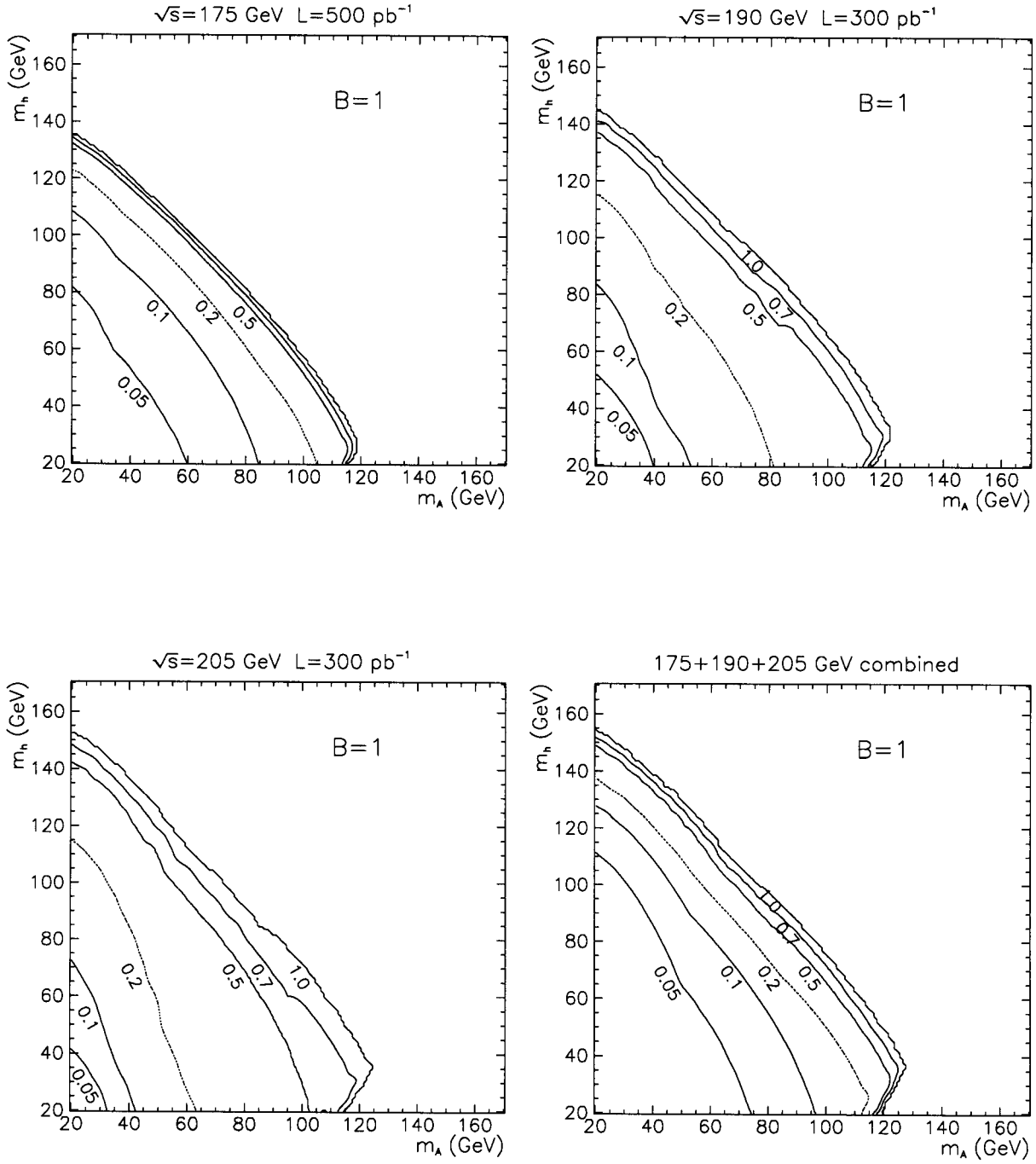

FIG. 4. Bounds on ϵ_A^2 as a function of M_h and M_A for $B=1$. The plots show the bounds obtained for $\sqrt{s}=175$, 190, and 205 GeV and the constraints obtained by combining all three expected LEP II runs. The allowed region of the parameter space is above the lines of constant ϵ_A.

$$c_A(M_h,M_A,B)\epsilon_A^2+c_B(M_h,M_A,B)\epsilon_B^2\leqslant n_0(M_h,M_A), \quad (31)$$

where the functions $c_{A(B)}$ can be obtained from Eqs. (27)–(30) and n_0 is the maximally allowed number of signal events, which depends on the background cross sections after cuts and on the confidence level. It is clear from the above expression that the weakest limits on ϵ_A (ϵ_B) can be obtained assuming $\epsilon_B=0$ ($\epsilon_A=0$). In fact, for given values of M_h, M_A, B, and n_0 the allowed region of the parameters ϵ_A and ϵ_B is the interior of an ellipse with semiaxes $\sqrt{n_0/c_A}$ and $\sqrt{n_0/c_B}$. Therefore, we present the limits on the semiaxes of this ellipse as a function of M_h, M_A for the two most interesting cases: $B=1$, i.e., fully invisible h decay, and weakest limits, obtained by varying B from 0 to 1.

For illustration, we exhibit in Table VI typical values of the 95% C.L. maximum number of signal events in each channel (n_0), assuming that the analysis is done for just one channel. These numbers should be taken with a grain of salt since they depend on the point of the parameter space due to the invariant mass cut.

In order to obtain constraints on ϵ_A (ϵ_B) combining the different final state topologies, we calculate the appropriate

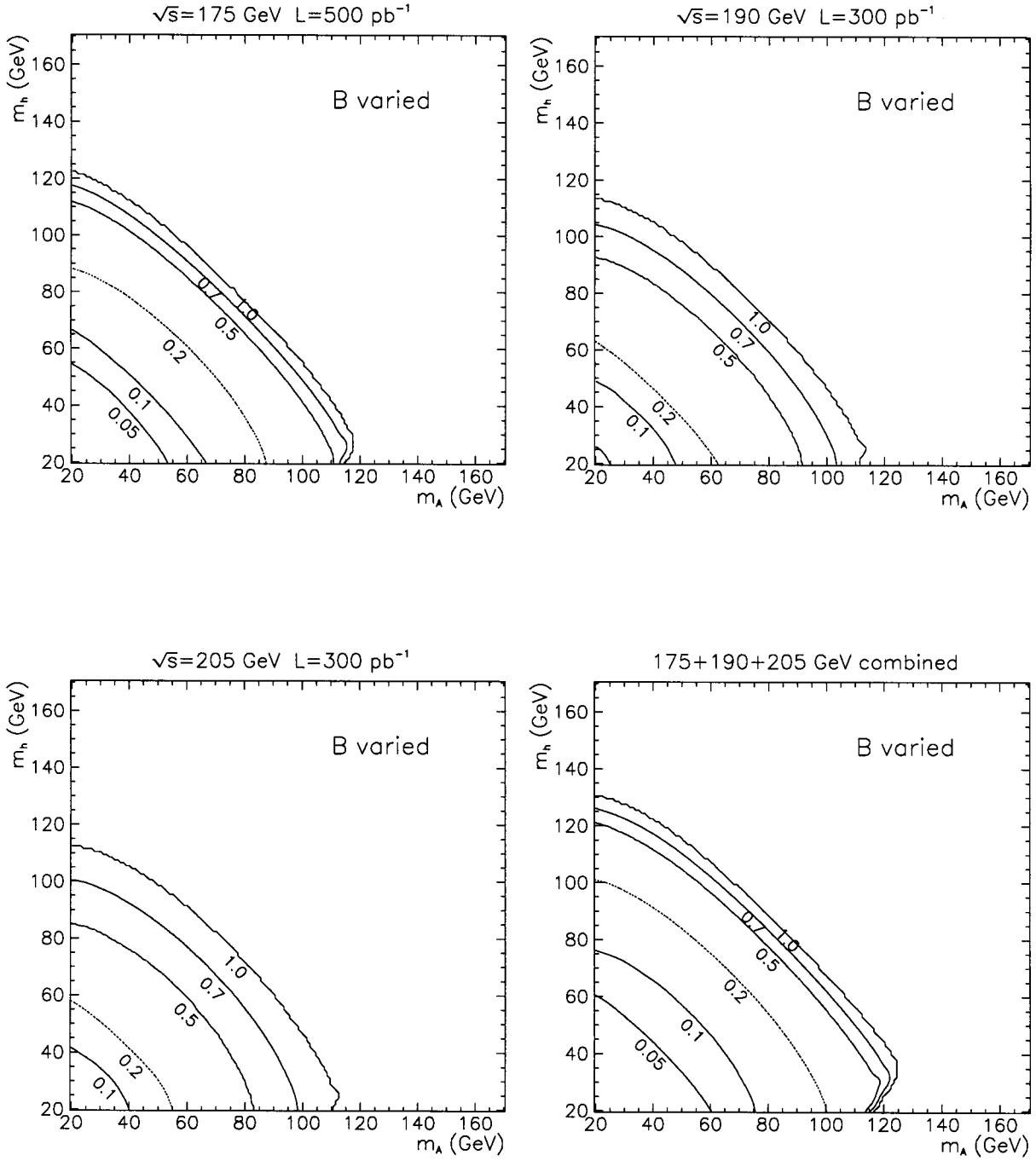

FIG. 5. B-independent bounds on ϵ_A^2 as a function of M_h and M_A. The plots show the constraints obtained for $\sqrt{s}=175$, 190, and 205 GeV and the combined bounds from all three expected LEP II runs.

exclusion confidence levels C.L.$_i$ for each channel separately, for a given value of ϵ_A (ϵ_B). Then, we evaluate the multichannel exclusion confidence level using the formulas

$$\text{C.L.}=1-(1-\text{C.L.}_1)\cdots(1-\text{C.L.}_n). \tag{32}$$

Finally, we choose as our limit for ϵ_A (ϵ_B) the value for which the combined C.L. is equal to 95%.

We start our analysis assuming that $\epsilon_A=0$, that is, we study the simplest model exhibiting invisibly decaying Higgs bosons, which is the one considered in Refs. [10,11]. In this model only one singlet scalar field is added to the SM Higgs doublet. We show in Fig. 3 the constraints on the coupling ϵ_B^2 with the excluded region of the parameter space at 95% C.L. being below the lines in this figure. The dotted (dashed) line stands for the constraints stemming from the $bb\not{p}_T$ channel for $B=0$ ($B=1$), while the dot-dashed curve represents the limits from the $\ell^+\ell^-\not{p}_T$ channel for $B=1$. We also exhibit in this figure an absolute bound on ϵ_B^2 (solid line) based on all channels together, including the visible h decays (25) and (26). The absolute bound is obtained by varying B in the range between 0 and 1 and taking the lowest bound on ϵ_B^2. The strongest single-channel constraint originates from the $bb\not{p}_T$ final state since there are many more signal events

with this topology, independently of the value of the branching ratio B. Moreover, the $\ell^+\ell^-\not{p}_T$ topology also exhibits a relatively large WW background. In fact, the analysis of the final state $bb\not{p}_T$ allows us to extend the results of Ref. [10]. Notice that for $B=0$ our limits are, in fact, on the SM Higgs boson mass and on its coupling to the Z. Indeed, our results are compatible to the ones obtained in Ref. [15].

The weakest and more solid constraints on ϵ_A are those obtained assuming $\epsilon_B=0$. Including all the final state topologies and assuming $\epsilon_B=0$ we obtain the bounds on ϵ_A^2 which are shown in Figs. 4 and 5. Even with this simplifying hypothesis, we are still left with the three-dimensional parameter space (M_A, M_h, ϵ_A). The absence of an invisible Higgs boson signal excludes the region above the lines of constant ϵ_A in Fig. 4, at 95% C.L. In this figure we exhibit the constraints on ϵ_A^2 obtained under the assumption that h decays exclusively into the invisible final state ($B=1$). Figure 5 contains the B-independent bounds on ϵ_A^2 obtained, as in the ϵ_B^2 case, by varying B in the range between 0 and 1 and keeping the weakest bound.

In general, the topologies (27) and (29) are dominated by the associated production, as long as they are not strongly suppressed by small ϵ_A couplings or by phase space. Therefore, for a given value of M_h, the constraints on the associated production coupling ϵ_A are stronger than those on ϵ_B^2 provided M_A is not very large. Another general feature of our results is that the final state $bb\not{p}_T$ (27) leads to the stronger limits on ϵ_A coupling than those given by the other topologies where h is decaying visibly, especially by $bbbb$ final state.

V. CONCLUSIONS

The Higgs boson can decay into a pair of invisible massless Goldstone bosons in a wide class of models in which a global symmetry, such as lepton number, is spontaneously broken. We performed a model-independent analysis of the capability of LEP II to probe for such a Higgs boson, assuming that it couples to the Z and a CP-odd scalar A, not analyzed before. We studied the final state topologies $bb\not{p}_T$, $\ell^+\ell^-\not{p}_T$, $\ell^+\ell^-bb$, and $bbbb$, taking into account the backgrounds and choosing the cuts so as to enhance the signal.

In the case that the invisible Higgs boson does not couple to the CP-odd scalar A ($\epsilon_A=0$), we found out that the strongest constraints on the parameter space come from the final state $bb\not{p}_T$. For masses M_h up to approximately 70 GeV, the planned run at $\sqrt{s}=175$ leads to the strongest limits due to its higher luminosity. On the other hand, the higher center-of-mass energy runs are needed to expand the range of masses that can be probed. The results of our complete analysis for this case extend the previous results of Ref. [10]. We also analyzed the extreme case $\epsilon_B=0$, in which the invisibly decaying Higgs boson does not couple to the Z. In this scenario, the strongest limits also come from the final state $bb\not{p}_T$. As a rule of thumb, the signal for the invisible Higgs boson being produced in association with A can be detected provided $M_h+M_A\lesssim 150$ (100) GeV for $\epsilon_A=1$ (0.1).

The invisibly decaying Higgs boson can also give rise to signals at the LHC, such as $\ell^+\ell^-\not{p}_T$ [18]. The invisible decay has good advantages over the standard model $h\to\gamma\gamma$ decay mode in the intermediate Higgs boson mass region, since its branching fraction can be large. Unfortunately, however, the ability to reconstruct the invisible Higgs boson mass is absent in the case of hadron collisions. This makes the signature of invisibly decaying Higgs bosons in e^+e^- collisions especially important and a crucial check of any signal that might be seen at the LHC. In this paper we have shown that LEP II will be able to unravel the existence of an invisibly decaying Higgs boson for a large fraction of the relevant parameter space. As a final remark we note that models with invisibly decaying Higgs bosons may lead to other interesting physical effects that could be detectable experimentally [19].

ACKNOWLEDGMENTS

We thank S. Katsanevas for useful discussions and for bringing Ref. [15] to our attention. This work was supported by the University of Wisconsin Research Committee with funds granted by the Wisconsin Alumni Research Foundation, by the U.S. Department of Energy under contract No. DE-FG02-95ER40896, by DGICYT under Grant No. PB92-0084, by Conselho Nacional de Desenvolvimento Científico e Tecnológico (CNPq/Brazil), by Fundacão de Amparo à Pesquisa do Estado de São Paulo (FAPESP/Brazil), and by the Alexander von Humboldt Stiftung. Work supported in part by EEC under TMR Contract No. ERBFMRX-CT96-0090.

[1] P. W. Higgs, Phys. Lett. **12**, 132 (1964); F. Englert and R. Brout, Phys. Rev. Lett. **13**, 321 (1964); G. Guralnik and C. K. Hagen, *ibid.* **13**, 585 (1964).

[2] F. Richard, in *Elementary Particle Physics: Present and Future*, Proceedings of Valencia 95, edited A. Ferrer and J. W. F. Valle (World Scientific, Singapore, 1996), pp. 3–31.

[3] Y. Chikashige, R. Mohapatra, and R. Peccei, Phys. Lett. **98B**, 265 (1980).

[4] For a review see J. W. F. Valle, Prog. Part. Nucl. Phys. **26**, 91 (1991), and references therein.

[5] A. Joshipura and J. W. F. Valle, Nucl. Phys. **B397**, 105 (1993); A. S. Joshipura and S. Rindani, Phys. Rev. Lett. **69**, 3269 (1992).

[6] J. E. Kim, Phys. Rep. **150**, 1 (1987), and references therein.

[7] F. de Campos and J. W. F. Valle, Phys. Lett. B **292**, 329 (1992); A. Masiero and J. W. F. Valle, *ibid.* **251**, 273 (1990); J. C. Romão, C. A. Santos, and J. W. F. Valle, *ibid.* **288**, 311 (1992).

[8] R. E. Shrock and M. Suzuki, Phys. Lett. **110B**, 250 (1982); J. D. Bjorken, in *The Project, the Progress, the Physics*, Proceedings of the Symposium on the SSC, Corpus Christi, Texas, 1991 (SSCL Report No. SR-1213, Corpus Christi, 1991).

[9] Higgs Physics at LEP2, convenors M. Carena and P. Zerwas *et al.*, to appear in the Proceedings of LEP2 Workshop, edited by G. Altarelli *et al.*, CERN Yellow Report No. hep-ph/9602250 (unpublished).

[10] A. Lopez-Fernandez, J. C. Romao, F. de Campos, and J. W. F. Valle, Phys. Lett. B **312**, 240 (1993).

[11] B. Brahmachari *et al.*, Phys. Rev. D **48**, 4224 (1993); ALEPH Collaboration, Phys. Lett. B **313**, 312 (1993); **313**, 299 (1993).

[12] O. J. P. Éboli, *et al.*, Nucl. Phys. **B421**, 65 (1994); F. de Campos *et al.*, in e^+e^- *Collision at 500 GeV: The Physics Potential*, Proceedings of the Workshop, Munich, Annecy, Hamburg, 1991, edited by P. Zerwas (DESY Report No. 92-123, Hamburg, 1992), p. 55.

[13] F. de Campos, M. A. Garcia-Jareño, A. S. Joshipura, J. Rosiek, D. P. Roy, and J. W. F. Valle, Phys. Lett. B **336**, 446 (1994).

[14] F. de Campos, O. J. P. Éboli, J. Rosiek, and J. W. F. Valle, Report No. MAD-PH 95-923, hep-ph/9512362 (unpublished).

[15] DELPHI Collaboration, Report No. DELPHI 95-57 PHYS 493 (unpublished).

[16] T. Sjöstrand, Comput. Phys. Commun. **82**, 74 (1994).

[17] K. Hagiwara *et al.*, Nucl. Phys. **B365**, 544 (1991); B. Mele and S. Ambrosiano, *ibid.* **B374**, 3 (1992).

[18] J. Gunion, Phys. Rev. Lett. **72**, 199 (1994); D. Choudhhury and D. P. Roy, Phys. Lett. B **322**, 368 (1994); J. C. Romão, F. de Campos, L. Diaz-Cruz, and J. W. F. Valle, Mod. Phys. Lett. A **9**, 817 (1994).

[19] J. W. F. Valle, in *Neutrino 92*, Proceedings of the The International Symposium on Neutrino Physics and Astrophysics, Granado, Spain, edited by A. Morales [Nucl. Phys. B (Proc. Suppl.) **31**, 221 (1993)].